Chemical Science

ROYAL SOCIETY OF CHEMISTRY

EDGE ARTICLE

View Article Online
View Journal | View Issue

Cite this: *Chem. Sci.*, 2025, **16**, 19762

All publication charges for this article have been paid for by the Royal Society of Chemistry

Received 13th June 2025
Accepted 19th September 2025

DOI: 10.1039/d5sc04331j

rsc.li/chemical-science

Temperature dependent luminescence of europium/cyanine FRET pairs

Tsz Lam Cheung and David Parker

The temperature dependence of light emission from three europium complexes has been examined in detail between 293 and 318 K in aqueous buffered solution. Each complex undergoes temperature dependent sensitised emission *via* an integral chromophore that possesses an ICT state, to which thermally activated reverse energy transfer occurs. In the presence of an energy matched FRET acceptor, emission from the Eu donor and the near-IR cyanine dye show different temperature variations of emission lifetime and intensity, paving the way for the development of optical temperature probes. The examples studied include an intramolecular europium-dye conjugate and FRET pairs based on Eu and cyanine dye conjugates of Vismodegib, the competitive antagonist for the Smoothened receptor in the Hedgehog signalling pathway. This study paves the way for the development of targeted optical temperature probes.

Introduction

Förster Resonance Energy Transfer (FRET) is a radiationless process between donor and acceptor molecules that takes place by a dipole–dipole interaction governed by the laws of quantum electrodynamics. It is used widely in natural science to estimate distances between two labelled sites, notably in molecular biology where FRET is a useful tool in quantifying molecular dynamics, *e.g.* for the study of protein–protein and protein–DNA interactions or to monitor time-dependent changes in protein conformation.[1]

FRET is not a thermally activated process characterised by an energy barrier. The rate of energy transfer is a function of the inverse sixth power donor–acceptor distance, and FRET efficiency is also determined by the magnitude of the spectral overlap integral between donor emission and acceptor absorption. It can be influenced by temperature dependent factors, such as luminophore thermal stability and the sensitivity of the donor excited state to non-radiative vibrational quenching.[2]

Stimulated by the clarification of temperature-dependent Eu luminescence in systems where back energy transfer occurs to a low-lying internal charge transfer (ICT) triplet state,[3] we hypothesised that it was timely to explore systems in which both donor and acceptor emission lifetimes and intensities are temperature dependent. In such a situation, it may be possible to define new FRET pairs in which key luminescence parameters, such as donor or acceptor lifetimes or differences in donor/acceptor emission intensities (or their ratio) could be used to calibrate local temperature, *e.g.* for temperature probe development, and for confocal microscopy or fluorescence lifetime imaging (FLIM) applications.[4,5]

Ideally, any optical thermometer should exhibit a high relative thermal sensitivity value S_r, reporting the relative change of the measured thermometric parameter (Δ) per unit temperature. The S_r parameter is independent of the nature of the thermometer, allowing direct comparison between different temperature probes; it is defined by eqn (1):

$$S_r = \frac{1}{\Delta}\left|\frac{\delta\Delta}{\delta T}\right| \quad (1)$$

where Δ is either the integrated area of the emission band or the emission lifetime.

FRET systems based on Eu(III) donors and a cyanine dye acceptor are widely used in commercial homogeneous time-resolved bioassays.[6–8] In these systems, the spectral overlap integral between a cyanine 647 dye acceptor, *e.g.* **1** (named 'Dy-647-CO_2^-'), and judiciously designed Eu(III) complexes with large $\Delta J = 2$ and small $\Delta J = 3$ and 4 emission bands, has been optimised to maximise FRET efficiency. Indeed, efficiency values of over 95% are common, with characteristic Förster radii (R_0) of around 7 nm estimated for the mean donor–acceptor distance in 50% efficient energy transfer.[9]

The cyanine dyes exhibit an intrinsic temperature-sensitive fluorescence, independent of any aggregation phenomenon.[10] In aqueous solution, lower temperatures give rise to higher fluorescence quantum yields associated with higher solvent viscosity, as well as a deceleration of the forward and reverse rates of *trans–cis* isomerisation that lead to the formation of non-emissive species.[11] Europium(III) complexes do not usually show a significant temperature dependence of their photoluminescence quantum yields. However, recent work with

Department of Chemistry, Hong Kong Baptist University, Kowloon Tong, Hong Kong, China

$[EuL^1]^-$ using transient absorption spectroscopy has defined the mechanism of sensitised emission at the sub-picosecond timescale, explaining the origins of the relatively steep temperature dependence (*ca* 10 μs K^{-1}) of the Eu emission lifetime.[3] Thermally activated back energy transfer was shown to occur from the $^5D_1$ and $^5D_0$ Eu excited states to the triplet excited state manifold of the internal charge transfer state (ICT) of the aryl-alkynyl-pyridyl chromophore.[12,13]

Accordingly, we have set out to examine the effect of temperature in the classical FRET system $[EuL^1]^-$/**1**, and in the covalently linked system, $[EuL^2]^-$ where the FRET process is most likely to be intramolecular, Chart 1. In addition, we have prepared the receptor-targeted FRET components, $[EuL^3]$ and the cyanine dye conjugate **3**. The targeting vector chosen was the competitive antagonist, Vismodegib **2**.[14]

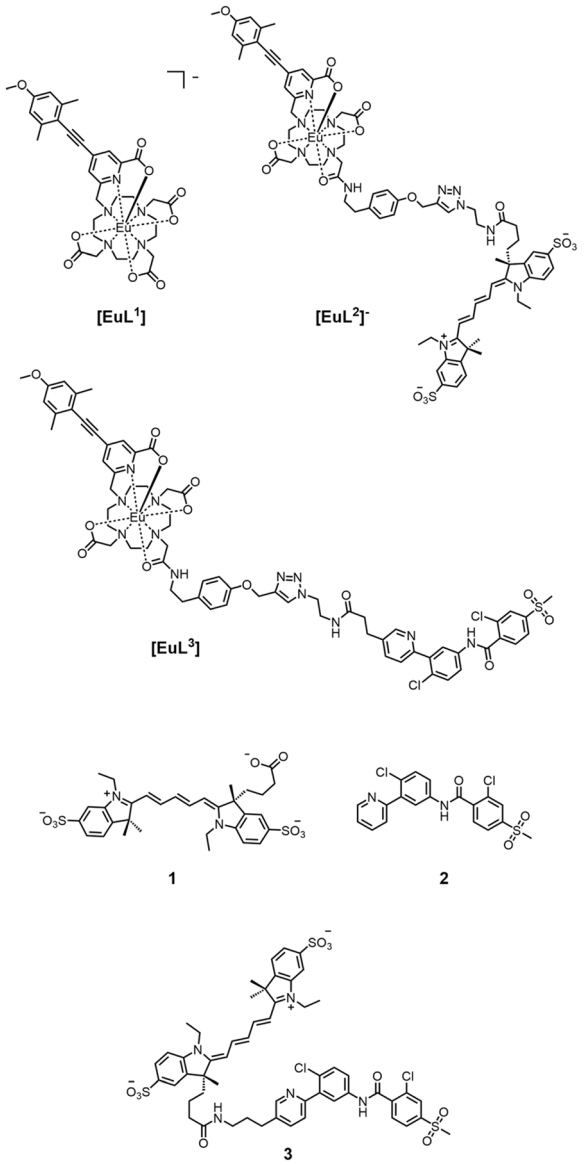

Chart 1 Structures of the Eu(III) complexes $[EuL^{1-3}]$, the cyanine dye Dy-647-CO_2^- **1**, competitive antagonist Vismodegib **2**, and cyanine dye conjugate **3**.

Vismodegib is an inhibitor of the Hedgehog signalling pathway, with an IC_{50} value of 3 nM. Its approval for use in humans was granted in 2012 by the Food and Drug Administration (FDA), for the treatment of basal-cell carcinoma and medulloblastoma.[14] It binds selectively to the key G-protein coupled receptor, Smoothened (SMO), a transmembrane GPCR essential for normal embryonic development and tissue homeostasis.[15] A key mechanism in tumorigenesis is believed to involve activation of the Hedgehog signalling pathway by SMO. In basal cell carcinoma, mutations in the Hedgehog pathway are believed to result in rapid proliferation of basal cells, and it has been found that perturbation of this pathway is relevant in >90% of basal cell carcinomas.

In parallel with a quest for the creation of targeted fluorescent probes for certain GPCRs,[16] and for purposes of comparison, the Vismodegib conjugate, $[EuL^3]$ and its FRET acceptor **3**, have been prepared as temperature sensitive components for receptor-targeted FRET bioassays. In each case, a relatively long spacer group has been introduced between the targeting vector and the luminescent moiety, in an effort to minimise the loss of affinity of the Vismodegib antagonist for the receptor binding site. Functionalisation of Vismodegib was made at the *meta* position in the pyridine group, following inspection of the PDB X-ray structure (5L7I) of the Vismodegib-Smoothened complex.[17] In doing so, we set out to minimise perturbation of the key hydrogen-bonding networks around the Vismodegib aryl and sulfonyl groups that stabilise the non-covalent adduct in the hydrophobic pocket.

Results and discussion

Details of the synthesis and characterisation of the Eu(III) complexes are reported in the SI. The anionic complex, $[EuL^1]^-$ was prepared according to the literature method,[3] and the other two complexes were prepared from a common alkyne intermediate, *via* a copper catalysed 'click' reaction with the appropriate azide. In every case, complexes and conjugates were purified by reverse phase HPLC, and selected photophysical data are summarised in Table 1 and Fig. S1–S4. The increase in the extinction coefficient of $[EuL^2]^-$ compared to $[EuL^1]$, is attributed to the overlap in the absorption spectra of the cyanine dye and the sensitising chromophore (Fig. S1). The fact that $[EuL^3]$ exhibits a higher ε value than the other two complexes and shows a 20 nm red shift, is suggestive of an intramolecular π–

Table 1 Selected photophysical properties for Eu(III) complexes and compound **3** (pH 7.4; 50 mM HEPES, 50 mM NaCl). Lifetime data were measured in water (5 μM complex, 295 K, λ_{exc} 355 nm)

Complex	τ/ms; (λ/nm)	λ_{abs} (nm)	Extinction coefficient (mM^{-1} cm^{-1})
$[EuL^1]^-$	0.81 (613)	346	16.4
$[EuL^2]^-$	0.18 (612)	349	20.8
		650	122
$[EuL^3]$	0.81 (612)	366	28.8
3	1.5×10^{-6} (670)	651	160

π* interaction between the aryl-alkynyl-pyrdiyl group and the Vismodegib aromatic system. No change in absorbance and ε values were found for a 200 fold variation in complex concentration.

In the rapid diffusion limit, transfer of energy from a long-lived donor to a freely diffusing acceptor (*i.e.* a quencher, *Q*) can be assumed to follow pseudo-first order kinetics, as shown in eqn (2)–(5), where τ_0 and τ represent emission lifetimes in the absence and presence of added quencher.[18]

$$1/\tau_0 = k_0 \quad (2)$$

$$1/\tau = k_{obs} \quad (3)$$

$$k_{obs} = k_0 + k_2[Q] \quad (4)$$

$$\tau_0/\tau = 1 + k_2/k_0[Q] = 1 + K_{SV}[Q] \quad (5)$$

Hence, a plot of τ_0/τ *vs.* $[Q]$ gives a straight line with a slope equal to $K_{SV} = k_2/k_0$. Assuming that the emission lifetime is directly proportional to the measured emission intensity, then I_o/I values can be used instead of emission lifetimes to allow estimates to be made of the second order rate constant for energy transfer k_2 (*i.e.* k_q) and its associated Stern–Volmer quenching constant, typically expressed as K_{SV}^{-1}.

The quenching of the Eu(III) complex, $[EuL^1]^-$ by the cyanine dye **1**, was examined by observing changes in the Eu(III) emission intensity at 613 nm as a function of acceptor concentration, over the range of 0.25 to 5 μM, using a 5 μM solution of the Eu(III) complex (Fig. 1). A clean isoemissive point was observed at 632 nm. The experimental data were fitted by linear regression analysis, according to a classical Stern–Volmer model, to give a second order quenching rate constant, $k_q = 1.8 \times 10^9$ M^{-1} s^{-1}, with a K_{SV}^{-1} value of 1.5×10^{-6} M. Very similar values have been reported previously for closely related Eu/cyanine dye FRET pairs, consistent with efficient energy transfer in each case.[9,19,20]

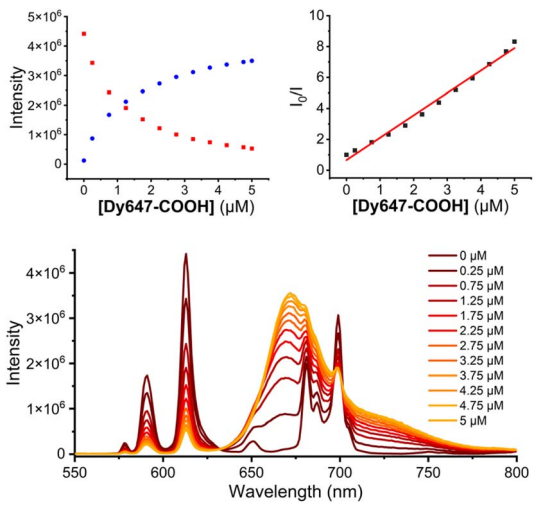

Fig. 1 (Lower) variation in emission spectral profiles for $[EuL^1]^-$ (5 μM) titrated with Dy-647-CO_2^-, **1** (0 to 5 μM, pH 7.4, 50 mM HEPES, 50 mM NaCl, 293 K, λ_{exc} 347 nm). (Upper right) plot of maximum emission intensity ratio at 613 nm for $[EuL^1]^-$ titrated with **1**; data fitted by linear regression gave a second order quenching rate constant, $k_q = 1.8 \times 10^9$ M^{-1} s^{-1}, with $K_{SV}^{-1} = 1.5 \times 10^{-6}$ M. (Upper left) changes in Eu emission (red: 613 nm) and dye emission intensity (blue: 671 nm) following incremental addition of the cyanine dye **1**.

Temperature dependence of intermolecular FRET between $[EuL^1]^-$ and 1

Both $[EuL^1]^-$ and the cyanine dye **1**, exhibit a pronounced temperature dependence of their emission lifetime and intensity. For the Eu complex, excitation at 355 nm gave rise to lifetime variations averaging −9.8(2) μs K^{-1} between 293 and 318 K, with little variation over the pH range 4.5 to 7.0. Parallel reductions in emission intensity were observed, with S_r values of 1.2 and 1.7% K^{-1} at 293 and 318 K. For the dye itself, the temperature variation following excitation at 632 or 640 nm was even larger, and the intensity fell by about a factor of two from 293 to 318 K, with corresponding S_r values of 1.9 and 3.7% K^{-1} (Fig. 2).

Next, the temperature dependences of the donor (D = Eu*) and acceptor (A = cyanine dye) emission profiles were examined for equimolar mixtures of $[EuL^1]^-$ and **1**, over the concentration range 0.3 to 5.0 μM. The temperature dependence of the IR dye emission at 670 nm differed, according to whether excitation occurred at 347 nm or 375 nm, exciting the Eu ion first *via* the sensitised emission pathway, or whether direct dye excitation occurred at 632 or 640 nm. By taking the difference in the measured 670 nm emission intensities, following successive excitation at 347 and 632 nm (or 375 and 640 nm), a linear dependence with temperature was found (Fig. 3).

This emission intensity difference, between the indirect FRET (D*/A to D/A*) and the direct excitation (A to A*) pathways (Fig. 3, right), presumably mainly arises from the temperature dependence of emission from the europium excited state, as Förster energy transfer is not thermally activated. Of course, the 670 nm emission intensity from the cyanine dye also intrinsically has a dependence on excitation wavelength. About two-thirds of the dye is directly excited at 632 and 640 nm, as deduced from the excitation profile. Moreover, the cyanine dye

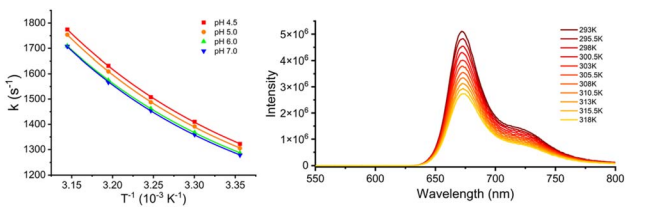

Fig. 2 (Right) temperature dependence of fluorescence emission from **1** (5 μM; λ_{exc} 632 nm, 50 mM NaCl, 50 mM HEPES, pH 7.4), for which the temperature coefficient averaged −9.8(2) μs K^{-1}, with relative thermal sensitivity parameter values, S_r of 1.9 and 3.7% K^{-1} at 293 and 318 K respectively; (left) variation of the europium emission lifetime with temperature at the stated pH values for $[EuL^1]^-$; proportionate changes in Eu emission intensity occurred; S_r values: 1.2 and 1.7% K^{-1} at 293 and 318 K. See Fig. S3 for the model used to fit the observed data.

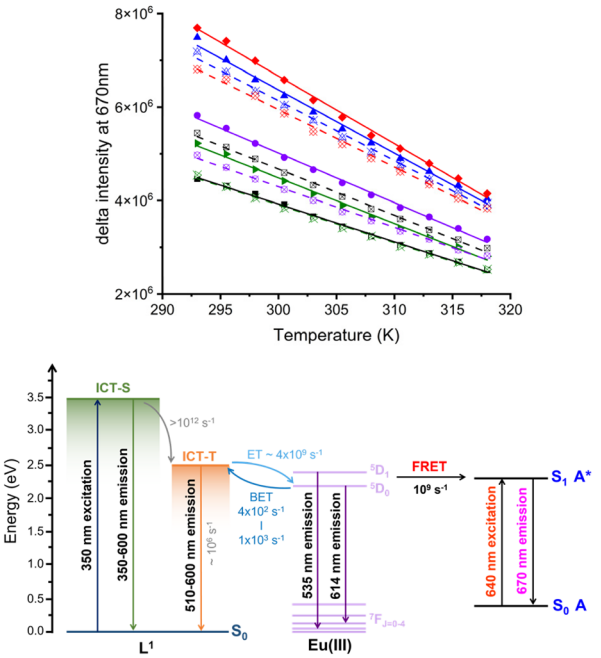

Fig. 3 (Upper) temperature variation of the emission intensity difference at 670 nm for equimolar mixtures at differing concentrations of the FRET pair, $[EuL^1]^-$ and **1**, (black: 5 μM; blue: 2.50 μM; red: 1.25 μM; olive: 0.62 μM; purple: 0.31 μM; solid: λ_{exc} 375 and 640 nm; dashed: λ_{exc} 347 and 632 nm). S_r values (293 K and 318 K) averaged 1.8/1.9 and 3.3/3.2% K^{-1} for 375/640 and 347/632 nm excitation pairs. (Lower) schematic depicting photophysical pathways in Eu sensitisation prior to FRET, leading to either 'indirect' (D*–A to D–A*) emission from the dye singlet excited state A*, or direct dye emission (A*– A).

has measurable absorbance in the range 340 to 380 nm (Fig. S1), so that it is also excited directly during sensitised emission of Eu (*ca* 2%). The co-excitation of Eu and the dye in $[EuL^1]^-$/**1** mixtures is revealed in the corresponding excitation spectra, recorded using 347 nm excitation, (Fig. S2), and by the observation of two emission lifetimes for the 670 nm emission: one in the nanosecond regime (*i.e.* direct dye fluorescence) and the other component in the 0.1 to 0.2 millisecond period, corresponding to the FRET pathway (Table S1 and Fig. 3).

The observed dye emission behaviour (Fig. 3, left) was characterised by S_r values at 293 K and 318 K averaging 1.8/1.9 and 3.3/3.2% K^{-1} for 375/640 and 347/632 nm excitation pairs, respectively. Apparent linear variations of lifetime or emission intensity with T were found, over the relatively short temperature range shown here (Fig. 3–7). We showed earlier that the Eu temperature variation exhibits a more complex exponential dependence of the rate of Eu decay with T^{-1}, (Fig. S3, plotting $\log k_{obs}$ *vs.* $1/T$) in agreement with an Arrhenius model, associated with thermally activated back energy transfer between the Eu $^5D_{1,0}$ excited states and the internal charge transfer excited state triplet manifold.[3]

Excitation wavelengths of 375 and 640 nm were chosen here, as they correspond to the laser sources used in the modern confocal microscopy set-ups that allow fast switching between different laser excitations, *e.g.* aided by an acousto-optic tuneable filter, as required for the hypothetical, rapidly-switched intensity difference method.

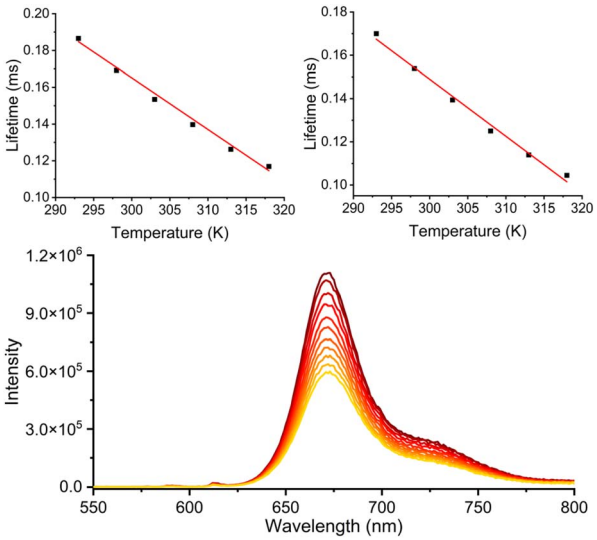

Fig. 4 (Upper left) variation of the Eu emission lifetime for $[EuL^2]^-$ (5 μM; λ_{em} 612 nm, λ_{exc} 355 nm) as a function of temperature (50 mM HEPES, 50 mM NaCl, pH 7.4); relative thermal sensitivity parameters, S_r were 1.5 and 2.5% K^{-1} at 293 and 318 K respectively. The experimental lifetime variation was −2.8 μs K^{-1}, compared to 9.8 μs K^{-1} for $[EuL^1]^-$. (Upper right) variation of the cyanine dye emission lifetime at 670 nm, (λ_{exc} 355 nm); the lifetime variation (slope −2.6 μs K^{-1}) echoes the Eu donor's behaviour. (Lower) reduction in luminescence from 293 to 318 K following excitation at 350 nm.

Temperature dependence of intramolecular FRET in $[EuL^2]^-$

In $[EuL^2]^-$ the Eu donor and cyanine dye acceptor are covalently linked and separated by 22 atoms, a distance of about 2 nm, notwithstanding the considerable conformational mobility of the chain separating the FRET pair. Following excitation of the chromophore at 355 nm (Fig. 4), Eu emission at 612 nm was barely visible and predominant dye emission at 670 nm was observed. Both the very weak Eu emission at 612 nm and the

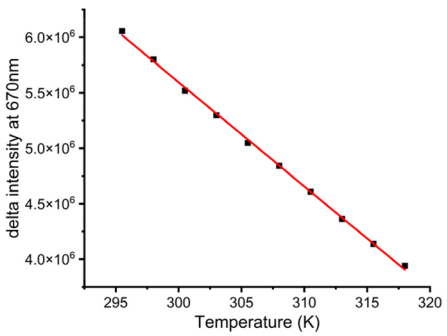

Fig. 5 Variation of the difference in emission intensity at 670 nm for $[EuL^2]^-$ (5 μM) as a function of temperature (50 mM HEPES, 50 mM NaCl, pH 7.4) following successive excitation at 350 and 632 nm; relative thermal sensitivity parameters, S_r values are 1.6 and 2.6% K^{-1} at 293 and 318 K respectively. Near identical (±0.1) values were measured after excitation at 375 and 640 nm.

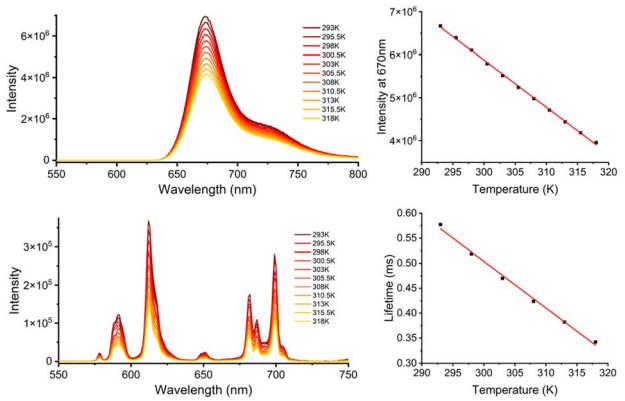

Fig. 6 (Upper left) changes in the emission spectrum of **3** with temperature; (upper right) variation of the emission intensity at 670 nm (5 μM; λ_{exc} 632 nm) as a function of temperature (50 mM HEPES, 50 mM NaCl, pH 7.4); relative thermal sensitivity parameter, S_r values, were 1.6 and 2.8% K^{-1} at 293 and 318 K, respectively; analysis of parallel lifetime variations gave S_r values of 1.4 and 2.1% K^{-1}. (Lower left) temperature variation of [EuL^3] emission; (lower right) change in the Eu emission lifetime at 612 nm as f(*T*) (−9.0 μs K^{-1}); (5 μM complex; λ_{exc} 362 nm; pH 7.4, 50 mM HEPES, 50 mM NaCl).

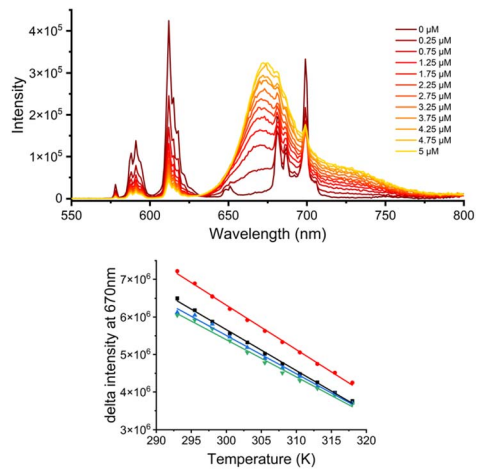

Fig. 7 (Upper) variation in observed emission for [EuL^3] (5 μM) titrated with **3** (0–5 μM, pH 7.4, 50 mM HEPES, 50 mM NaCl, 293 K, λ_{exc} 362 nm) highlighting the FRET process, characterised by an isoemissive point at 632 nm; $k_q = 1.6 \times 10^9$ M^{-1} s^{-1} and $K_{SV}^{-1} = 2.0 \times 10^{-6}$ M. (Lower) variations in the emission intensity difference at 670 nm for 5 : 5 and 20 : 5 μM concentrations of the FRET pair, [EuL^3] and **3** (red/green: λ_{exc} 375 and 640 nm; blue/black: λ_{exc} 362 and 632 nm). The S_r values at 293 K and 318 K averaged 1.7/1.6 and 2.9/2.8% K^{-1} for the 375/640 and 362/632 nm excitation pairs, respectively.

intense dye emission at 670 nm possessed a lifetime of between 0.1 to 0.2 milliseconds, consistent with a very efficient intramolecular FRET process, with emission from the dye acceptor echoing the lifetime of the Eu donor. The temperature coefficient for the lifetime reduction was the same in each case, averaging −2.8(2) μs K^{-1}.

In this example, the observed Eu emission intensity is too weak to allow a reliable ratiometric method (*e.g.* I_{613}/I_{670} nm) to be used to calibrate temperature. However, the intensity difference of the 670 nm dye emission, following successive excitation at 632 and 670 nm (or 375 and 640 nm, *vide supra*), could be used (Fig. 5), as in the example above with [EuL^1]$^-$ and **1** (Fig. 3). The measured S_r values in this case were 1.6 and 2.6% K^{-1} at 293 and 318 K, respectively.

Temperature dependent behaviour of a targeted, energy matched FRET pair, [EuL^3] and 3

A similar set of experiments to those described above was undertaken to define the temperature dependence of emission intensity and lifetime for the dye acceptor **3**, the europium complex donor, [EuL^3] and equimolar mixtures of **3** and [EuL^3], over the concentration range 5.0 to 0.3 μM, and at different excitation wavelengths (Fig. 6, 7 and Table 2). For the individual components, parallel temperature dependent behaviour was found to that observed with [EuL^1]$^-$ and **1** (Fig. 6). Lifetime variations in the nanosecond regime for the emission of the IR-dye at 670 nm,[11,21] following excitation at 340 nm where the dye also has measurable absorbance, are given in the SI (Table S1, Fig. S6 and S7).

With the FRET pair, **3** and [EuL^3] (Fig. 7), once again the difference in emission intensity at 670 nm of the dye acceptor could be used after pulsed excitation of the Eu complex at 362 or 375 nm, followed by direct excitation of the dye at 632 or 640 nm. The temperature coefficients for lifetime variation and corresponding thermal sensitivity parameters are collated in Table 2 (Fig. S5–S7 and Table S1 for additional nanosecond lifetime data). It is striking that very similar behaviour is exhibited for each FRET pair, with the targeted example based on Vismodegib giving rise to the largest S_r values overall, based on lifetime variation.

A series of experiments was then carried out in the presence of bovine serum albumin (BSA), to model what may occur in the case of non-specific protein binding of the Eu complex, for example *in cellulo*. Incremental addition of BSA to [EuL^3] at 295 K (pH 7.4) gave rise to an enhancement in europium emission intensity of a factor of six, without variation in spectral form, consistent with no change in the primary Eu coordination environment (Fig. S5).[22] A log *K* value of 5.09(5) was estimated for 1 : 1 protein association from the observed intensity variation, using non-linear least squares data analysis. With the cyanine dye conjugate **3**, no change in emission intensity was

Table 2 Lifetime variations with temperature for Eu complexes, and corresponding thermal sensitivity parameters (5 μM complex; pH 7.4; 50 mM HEPES, 50 mM NaCl); values refer to emission from Eu at 612 nm and, in parentheses, from the dye at 670 nm. For the cyanine dye **1**, S_r (293 K) = 1.9% K^{-1} and S_r (318 K) = 3.7% K^{-1}

Complex	Lifetime variation (μs K^{-1})	S_r (293 K) (% K^{-1})	S_r (318 K) (% K^{-1})
[EuL^1]$^-$	−9.8	1.2	1.7
[EuL^1]$^-$ + **1**	−2.7 (−2.6)	1.4 (1.4)	2.1 (2.0)
[EuL^2]$^-$	−2.8	1.5	2.5
[EuL^3]	−9.0	1.6	2.8
[EuL^3] + **3**	−2.3 (−2.2)	2.1 (2.0)	4.2 (4.1)

observed when adding BSA, suggesting that protein binding is very weak, as it is with **1**.

In the presence of a twenty-fold excess of BSA (0.1 mM), the Eu emission intensity in [EuL^3] fell by 30% as the temperature was reduced from 293 to 318 K. However, for a 1 : 1 mixture of [EuL^3] and **3**, (5 μM) in the presence of BSA (0.1 mM), the Eu emission intensity at 612 nm following excitation at 362 or 375 nm, diminished by a factor of two from 293 to 318 K, while dye emission at 670 nm fell by only 25% (Fig. S8). Such differential thermal sensitivity augurs well in seeking calibration methods for real-life situations, where FRET occurs rapidly from the Eu donor to the acceptor dye conjugate, when receptor-bound and within *ca* 10 nm of each other (R_0 values are typically 6 to 7 nm).

Conclusions

The temperature dependences of emission lifetime and intensity have been defined in the range 293 to 318 K for the three europium complexes and their energy/spectrally matched cyanine dye acceptors. In each case, efficient FRET was observed, characterised by formation of an isoemissive point at 632 nm. The lifetimes and emission intensities decrease as temperature rises in an approximately linear manner over the physiological range, and the lifetime of the FRET acceptor in the millisecond range has a temperature dependence that echoes its Eu donor, with S_r values in the range 1 to 3% K^{-1}. Such thermal sensitivity factors compare favourably with the wide range of molecular and supramolecular optical probes examined recently.[3–5]

Each europium complex can be excited selectively *via* the ligand ICT transition, following absorption of light by the alkynyl chromophore between 340 and 375 nm. Over this wavelength range, the cyanine dye also absorbs weakly. Indeed, its emission spectrum is characterised by two components, one in the nanosecond regime arising from direct excitation with a longer-lived component arising following energy transfer from the parent Eu donor. By taking the difference in emission intensity at 670 nm after sequential excitation at 347/632 nm or 375/640 nm, a linear calibration curve was obtained for the differential temperature response (Fig. 3, 5, 7 and Table 2), with S_r values of between 1.5 to 3% K^{-1}.

GPCR activity is known to be temperature dependent, *via* changes in membrane fluidity and protein dynamics, altering receptor activation. The GPCR 'Smoothened' is aberrantly activated in many cancers, leading to uncontrolled cell proliferation. Temperature induced stress may potentially modulate this activation, either enhancing or suppressing its signalling, according to the cellular context. Future experiments with the Vismodegib conjugates, **3** and [EuL^3] will be undertaken in cells possessing over-expressed Smoothened (SMO) cell surface receptors, comparing behaviour to normal controls. The feasibility of observing FRET in live cells will be assessed between a covalently labelled Eu-Vismodegib conjugate, attached for example using SNAP-Tag methods,[6,7] and a freely diffusing cyanine-Vismodegib conjugate, *e.g.* **3**. Such a process requires that a sufficiently high receptor density of the SMO receptor is present to outcompete non-specific probe binding,[7] and that the Vismodegib conjugate retains sufficient avidity to bind selectively to the SMO receptor on the cell surface. Given that time-resolved FRET microscopy on related Eu/cyanine dye systems has already been reported,[7] the differing temperature dependences of Eu and dye emission should assist in working out a temperature calibration protocol *in situ*.

Author contributions

The project was conceived by DP and the manuscript was written by DP and TLC; TLC carried out the synthesis and characterisation, the measurements of binding constants and the calculation of rate constants and lifetimes.

Conflicts of interest

There are no conflicts to declare.

Data availability

This manuscript contains primary data that is available in the SI or can be sought by request by writing to the corresponding author. Supplementary information is available containing details of synthesis, photophysical measurements and characterisation methods. See DOI: **https://doi.org/10.1039/d5sc04331j**.

Acknowledgements

DP thanks the Hong Kong Jockey Club Charities Trust for equipment support and the Hong Kong Government and Hong Kong Baptist University for support under the Global STEM Professorship scheme. TLC thanks Hong Kong Baptist University for studentship support.

Notes and references

1 L. Yuan, W. Lin, K. Zheng and S. Zhu, FRET-Based small molecule fluorescent probes: rational design and bioimaging applications, *Acc. Chem. Res.*, 2013, **46**, 1462–1473, DOI: **10.1021/ar300273v**.

2 H. Sahoo, Förster resonance energy transfer – spectroscopic nanoruler: principle and applications, *J. Photochem. Photobiol., C*, 2011, **12**(1), 20–30, DOI: **10.1016/j.jphotochemrev.2011.05.001**.

3 T. L. Cheung, Z. Ju, W. Zhang, D. Parker and R. Deng, Mechanistic investigation of sensitised europium luminescence: excited state dynamics and luminescence lifetime thermometry, *ACS Appl. Mater. Interfaces*, 2024, **16**, 43933–44394, DOI: **10.1021/acsami.4c06899**.

4 J. Zhou, B. del Rosal, D. Jaque, S. Uchiyama and D. Jin, Advances and challenges for fluorescence nanothermometry, *Nat. Methods*, 2020, **17**, 967–980, DOI: **10.1038/s41592-020-0957-y**.

5 K. Xue, C. Wang, J. Wang, S. Lv, B. Hao, C. Zhu and B. Z. Tang, A sensitive and reliable organic fluorescent

nanothermometer for non-invasive temperature sensing, *J. Am. Chem. Soc.*, 2021, **143**(35), 14147–14157, DOI: **10.1021/jacs.1c04597**.

6 A. Emami-Nemini, T. Roux, M. Leblay, E. Bourrier, L. Lamarque, E. Trinquet and M. J. Lohse, Time-resolved fluorescence ligand binding for G protein–coupled receptors, *Nat. Protoc.*, 2013, **8**, 1307–1320, DOI: **10.1038/nprot.2013.073**.

7 M. Delbianco, V. Sadovnikova, E. Bourrier, G. Mathis, L. Lamarque, J. M. Zwier and D. Parker, Bright, highly water-soluble triazacyclononane europium complexes to detect ligand binding with time-resolved FRET microscopy, *Angew Chem. Int. Ed. Engl.*, 2014, **53**, 10718–10722, DOI: **10.1002/anie.201406632**.

8 H. E. Rajapakse, N. Gahlaut, S. Mohandessi and L. W. Miller, Time-resolved luminescence resonance energy transfer imaging of protein–protein interactions in living cells, *Proc. Natl. Acad. Sci.*, 2010, **107**(31), 13582–13587, DOI: **10.1073/pnas.1002025107**.

9 D. Parker, J. D. Fradgley, M. Delbianco, M. Starck, J. W. Walton and J. M. Zwier, Comparative analysis of lanthanide excited state quenching by electronic energy and electron transfer processes, *Faraday Discuss.*, 2022, **234**, 159–174, DOI: **10.1039/D1FD00059D**.

10 J. Widengren and P. Schwille, Characterisation of photoinduced isomerisation and back-isomerisation of the cyanine dye Cy5 by fluorescence correlation spectroscopy, *J. Phys. Chem. A*, 2000, **104**, 6416–6428, DOI: **10.1021/jp000059s**.

11 A. Vahdani, M. Moemeni, D. Holmes, R. R. Lunt, J. E. Jackson and B. Borhan, Mechanistic Insight into the Thermal "Blueing" of Cyanine Dyes, *J. Am. Chem. Soc.*, 2024, **146**, 19756–19767, DOI: **10.1021/jacs.4c02171**.

12 M. Soulie, F. Latzko, E. Bourrier, V. Placide, S. J. Butler, R. Pal, J. W. Walton, P. L. Baldeck, B. Le Guennic, C. Andraud, J. M. Zwier, L. Lamarque, O. Maury and D. Parker, Comparative analysis of conjugated alkynyl chromophore-triazacyclononane ligands for sensitized emission of europium and terbium, *Chem.–Eur. J.*, 2014, **20**, 8636–8646, DOI: **10.1002/chem.201402415**.

13 S. J. Butler, M. Delbianco, L. Lamarque, B. K. McMahon, E. R Neil, R. Pal, D. Parker, J. W Walton and J. M Zwier, EuroTracker dyes: design, synthesis, structure and photophysical properties of very bright europium complexes and their use in bioassays and cellular optical imaging, *Dalton Trans.*, 2015, **44**, 4791–4803, DOI: **10.1039/c4dt02785j**.

14 A. Sekulic, M. R. Migden, A. E. Oro, L. Dirix, K. D. Lewis, J. D. Hainsworth, J. A. Solomon and A. Hauschild, Efficacy and safety of Vismodegib in advanced basal cell carcinoma, *N. Engl. J. Med.*, 2012, **366**, 2171–2179, DOI: **10.1056/NEJMoa1113713**.

15 A. M. Arensdorf, S. Marada and S. K. Ogden, Smoothened regulation, a tale of two signals, *Trends Pharmacol. Sci.*, 2015, **37**, 62–72, DOI: **10.1016/j.tips.2015.09.001**.

16 P. A. Insel, K. Sriram, M. W. Gorr, S. Z. Wiley, A. Michkov, C. Salmeron and A. M. Chinn, GPCRomics: an approach to discover GPCR drug targets, *Trends Pharmacol. Sci.*, 2019, **40**, 378–387, DOI: **10.1016/j.tips.2019.04.001**.

17 E. F. X. Byrne, R. Sircar, P. S. Miller, G. Hedger, G. Luchetti, S. Nachtergaele, M. D. Tully, L. Mydock-McGrane, D. F. Covey, R. P. Rambo, M. S. P. Sansom, S. Newstead, R. Rohatgi and C. Siebold, Structural basis of Smoothened regulation by its extracellular domains, *Nature*, 2016, **535**, 517–522, DOI: **10.1038/nature18934**.

18 C. F. Meares and T. G. Wensel, Metal chelates as probes of biological systems, *Acc. Chem. Res.*, 1984, **17**, 202–209.

19 W. Zhang, J. Li, H. Lei and B. Li, Forster resonance energy transfer from upconversion nanoparticles to quantum dots, *Opt. Express*, 2020, **28**, 12450, DOI: **10.1364/oe.386601**.

20 J. Vuojola, I. Hypannen, M. Nummela, J. Kankare and T. Soukka, Distance and temperature dependence in non-overlapping and conventional Forster resonance energy transfer, *J. Phys. Chem. B*, 2011, **115**, 13685–13694, DOI: **10.1021/jp.205564n**.

21 H. Lee, M. Y. Berezin, M. Henary, L. Strekowski and S. Achilefu, Fluorescence lifetime properties of near-infrared cyanine dyes in relation to their structures, *J. Photochem. Photobiol., C*, 2008, **200**, 438–444, DOI: **10.1016/j.jphotochem.2008.09.008**.

22 D. Parker, J. D. Fradgley and K.-L. Wong, The design of luminescent lanthanide probes and sensors, *Chem. Soc. Rev.*, 2021, **50**, 8193–8213, DOI: **10.1039/d1cs00310k**.